Food Innovation and Advances

ARTICLE

Open Access

https://doi.org/10.48130/fia-0026-0046

Food Innovation and Advances **2026**, 5(4): 563–577

Influence of γ-irradiation and vacuum concentration on microbial compositions and shelf-life qualities of gallnut honey: a comparative study by multi-omics

Xinyu Zhou[1,2], Xiaohui Mo[1,2], Wei Xu[1,2], Yingtong Li[1,2], Xiaoping Yang[3], Zhixin Wang[3], Kai Zhong[3], Qi Sun[4], Lirong Jia[1,2] and Feixia Duan[1,2*]

[1] *Department of Food Engineering, College of Biomass Science and Engineering, Sichuan University, No. 24 South Section 1, Yihuan Road, Chengdu 610065, China*
[2] *The Key Laboratory of Food Science and Technology of Ministry of Education of Sichuan Province, Sichuan University, Chengdu 610065, China*
[3] *Zhongjin irradiation Chengdu Co. Ltd., Chengdu 611930, China*
[4] *Washington State University, School of Food Science, Pullman, WA 99164, USA*
* Correspondence: duanfeixia@126.com (Duan F)

Abstract

Apis cerana Fabricius-produced gallnut honey (GH) is a geographically indicated product from Fengtong, Sichuan, China. The microbial composition and characteristic flavor substances of honey subjected to γ-irradiation and vacuum concentration treatment (VCT) were systematically compared to uncover the influence of pretreatment on honey shelf-life qualities. The high-throughput sequencing and colony counting suggested that, although honeybee- and pollen-originating probiotics (*Apilactobacillus* and *Bombella*) dominated fresh-collected GH, *Enterococcus*, *Methylobacterium*, *Clostridium*, *Faecalibacterium* and osmotolerant yeasts (*Hanseniaspora* and *Zygosaccharomyces*) jointly caused spoilage. These spoilage-associated taxa showed tolerance to VCT-caused low moisture-content, but were almost controlled by γ-irradiation (8 kGy). Sensory evaluation, HS-SPME-GC-MS, and HS-GC-IMS detection demonstrated that phenylacetaldehyde, isophorone, phenylethanol, dodecanal, lilac aldehyde, and esters were the characteristic flavor substances in GH. VCT caused significant loss of these fragrances with slight flavor deterioration. In contrast, γ-irradiation maintained GH aroma and inhibited undesirable volatile organic compounds (VOCs) possibly associated with microbial or enzymatic transformation, although it induced undesirable VOCs possibly associated with lipid peroxidation and Maillard-related pathways.

Keywords: Gallnut honey, Microbial composition, Flavor ingredients, High-throughput sequencing, Vacuum concentration, γ-irradiation, VOCs, GC-IMS

Citation: Zhou X, Mo X, Xu W, Li Y, Yang X, et al. 2026. Influence of γ-Irradiation and Vacuum Concentration on Microbial Compositions and Shelf-life Qualities of Gallnut Honey: A Comparative Study by Multi-omics *Food Innovation and Advances* 5(4): 563–577 https://doi.org/10.48130/fia-0026-0046

Introduction

Honey has long been popular with humans and widely consumed around the world, for its dual role as both a natural sweetener with uniquely pleasant aroma and a functional food with various health benefits[1]. As a mixture, honey is mainly composed of monosaccharides (over 70%) containing fructose and glucose, disaccharides such as sucrose and maltose, along with water (less than 20%), and numerous trace substances, including enzymes (α-amylase, α-glucosidase, glucose oxidase, and catalase), peptides, amino acids, phenolic compounds, carotenoids, terpenoids, minerals, vitamins, pigments, and volatile substances[2,3]. Due to its high osmotic pressure, low moisture content, and inherent antimicrobial agents, such as hydrogen peroxide (H_2O_2), methylglyoxal (MGO), bee defensin-1, and some specific phenolic compounds[4,5], honey was commonly considered a long-lasting food[6]. However, honey-contained food products induced food poisoning incidents caused by microorganisms and their toxic metabolites kept emerging[6–8]. In fact, the presence and proliferation of microorganisms in honey have been reported previously, and varieties of bacteria and spores, such as *Bacillus*, *Clostridium*, *Listeria spp*., *Acinetobacter,* and *Micrococcus*[9,10], as well as yeasts and molds, were isolated from honey[11]. Because of the broad sources of honey microorganisms, including the bee's digestive tract of pollens, environmental constituents (soil, air, water, etc.), and the collecting process, the microbial composition in honey and their proliferation in storage remained unclear and needed to be revealed more precisely for honey and honey-contained food products' hazard control[7,12].

Low-temperature vacuum concentration treatment (VCT) is still the most commonly used industrial strategy for honey shelf-life maintenance by maintaining low water contents, but with uncertain microbial risks. To control microbial proliferation in honey, several sterilization techniques, including ultra-high-temperature (UHT) sterilization, high-pressure sterilization, and microwave treatment[2,13], has been studied, while the negative impact on heat-sensitive bioactive components, flavor substances, and sensory attributes restricted their applications in honey. ^{60}Co-γ irradiation, as a safe and reliable non-thermal food sterilization treatment with strong penetration, low operating temperature, and few residues[14], could possess potential application value in microorganism risk control in honey products, and some previous study reported that γ-irradiation at 5–10 kGy reduced the total viable counts (TVC) in honey to un culturable levels, with no significant impacts on ash content, reducing sugars, pH value, viscosity, or rheological behavior[15]. However, irradiation usually induces free radical reactions that alter the chemical composition of foods, thereby affecting their flavor profile and active ingredients[16]. Accordingly, the sensory characteristics, flavor compounds, and non-volatile components in honey after γ-irradiation need systematic study.

The present work evaluated the microbial decontamination efficiency of γ-irradiation in the August-harvested gallnut honey (GH), which had relatively higher microbial loads. Furthermore, by

© The Author(s)

https://doi.org/10.48130/fia-0026-0046

comparing with VCT, the immediate and post-storage influence of γ-irradiation on GH sensory properties, microbial composition, and critical flavor substances was investigated, using sensory evaluation, high-throughput sequencing, headspace solid phase microextraction (HS-SPME) combined with gas chromatography-mass spectrometry (GC-MS), and headspace sampling coupled with GC-ion mobility mass spectrometry (HS-GC-IMS).

Materials and methods

Chemicals and reagents

Sodium chloride (AR, 99.5%), acetic anhydride (AR, 99%), concentrated sulfuric acid (AR, 98%), 2-octanol (GC, ≥ 99.5%), 2-methyl-3-heptanone (GC, ≥ 95%), and acetonitrile (HPLC, ≥ 99.9%) were supplied by Macklin Biochemicals (Shanghai, China). Culture media for microbial enumeration were supplied by Aoboxing Bio-Technology Co., Ltd. (Beijing, China), with specifics provided in Supplementary Table S1. C7–C40 n-alkanes mixed standard and C4–C9 n-ketones mixed standard were purchased from Aladdin Biochemicals (Shanghai, China). Ultrapure water was prepared by a KMCR-20 laboratory ultrapure water system (Chengdu Haochun Instrument Equipment Co., Ltd., Sichuan, China).

Sample collection and nectar-source identification

The honey samples utilized in this experiment, including gallnut honey (GH, from August to September), high-altitude multifloral honey (HMH, from September to October), low-altitude multifloral honey (LMH, from September to October), and rape honey (RH, from March to April), were collected in Fengtong Area, Wanyuan, Sichuan province, China. For each honey type, approximately 2 kg of honey was collected, and the sampling covered eight apiary sites in total. The samples included three independent batches, with each batch considered as one biological replicate and analyzed in triplicate as technical replicates. All samples were transported under cold chain conditions to Zhongjin Irradiation Chengdu Co., Ltd. (Chengdu, China) for irradiation and then transported to Sichuan University (Chengdu, China), where the study was carried out, and then stored at −80 °C in the dark until analysis. The nectar sources of each sample were identified by palynological analysis using a FESEM system (Nova Nano450, FEI, USA; Supplementary Fig. S1).

γ-Irradiation

GH was portioned into 30 g aliquots and packaged by heat sealing separately in food-grade PA/PE (polyamide/polyethylene) composite bags for subsequent use. Then, the packaged honey samples were irradiated with ^{60}Co-γ at Zhongjin Irradiation Chengdu Co., Ltd. (Chengdu, China) using a cobalt-60 irradiator (IV, BFT, China) at 4.0 (IS4), 6.0 (IS6), and 8.0 kGy (IS8). Irradiation was carried out at ambient temperature (approx. 25 °C) with a dose rate of 1.0 kGy/h. These irradiation doses were selected based on the standardized commercial microbial decontamination procedure provided by the irradiation facility.

Vacuum concentration treatment (VCT)

GH was vacuum concentrated using a rotary evaporator (N-1300VH-WB, EYELA, Japan) at 50 °C under 100 mbar for 60–80 min to achieve a water content of less than 20% (Supplementary Table S2). These conditions were selected based on preliminary trials, in which this temperature-pressure-time combination effectively reduced the moisture content to below 20% while avoiding excessive thermal treatment. The target moisture level was chosen according to the generally accepted moisture requirement for honey. The honey moisture content was determined using a handheld refractometer (DELIXI ELECTRIC, China) according to previous methods[17].

Accelerated storage

Honey samples (GH, IS4, IS6, IS8, and VCT) were packaged in PA/PE composite bags (30 g per aliquot, n = 3), incubated at 37 ± 1 °C and 55% ± 5% relative humidity for 0, 5, and 10 d, and subsequently transferred to −80 °C storage until analysis.

Microbial counts assay

In accordance with the microbial limits, testing, and enumeration methods stipulated in Chinese standard (GB 14963-2011) for honey, the following microbial parameters were analyzed in the honey samples: total aerobic microbial count, coliforms, molds, osmophilic yeasts, *Salmonella*, *Shigella*, and *Staphylococcus aureus*.

High-throughput sequencing

DNA extraction and PCR amplification

Total microbial genomic DNA was extracted from honey samples (GH-0, GH-10, VCT-0, VCT-10, IS8-0, and IS8-10, with three independent biological replicates for each condition) using a DNA extraction kit (Omega Bio-Tek, Norcross, GA, USA) following the manufacturer's protocol[18]. The quality and concentration of the DNA were assessed via 1.0% agarose gel electrophoresis and a NanoDrop 2000 spectrophotometer (Thermo Scientific, USA). The DNA was then stored at −80 °C for subsequent analysis. The V3–V4 hypervariable region of the bacterial 16S rRNA gene and the ITS1 region of the fungal ITS gene were amplified using the primer pairs 338F/806R[19] (5′-ACTCCTACGGGAGGCAGCAG-3′/5′-GGACTACHVGGGTWTCTAAT-3′) and ITS1F/ITS2R[20] (5′-CTTGGTCATTTAGAGGAAGTAA-3′/5′-GCTG CGTTCTTCATCGATGC-3′), respectively, with a thermal cycler PCR system (GeneAmp 9700, ABI, USA). The PCR products were verified by 2% agarose gel electrophoresis, purified using a PCR purification kit (YuHua, Shanghai, China), and quantified with the QuantiFluor™-ST system (Promega, USA).

High-throughput sequencing and data processing

Paired-end sequencing was performed on the Illumina MiSeq PE300 platform (Illumina, San Diego, USA) at Majorbio Bio-Pharm Technology Co., Ltd. (Shanghai, China). Raw reads were processed using Fastp (v.0.23.4) and FLASH (v.1.2.11) for demultiplexing, quality filtering, and merging. Quality-filtered sequences were denoised using the DADA2 plugin in QIIME 2 (v.2024) to generate amplicon sequence variants (ASVs). Sequences annotated as chloroplasts or mitochondria were removed, and all samples were rarefied to the same sequencing depth based on the sample with the fewest sequences. Taxonomic assignment of ASVs was conducted using the Naive Bayes classifier in QIIME 2 with the SILVA 16S rRNA database (v.138) for bacteria and the UNITE ITS database (v.8) for fungi. All bioinformatic analyses, including assessments of microbial alpha diversity, beta diversity, and differential abundance, were performed on the Majorbio Cloud Platform (https://cloud.majorbio.com). The raw data of 16S rRNA and ITS amplicon sequencing obtained in this study have been submitted to NCBI (National Center for Biotechnology Information) under accession number PRJNA1457969.

Sensory evaluation

The sensory characteristics of various honey samples were evaluated by a panel of 30 trained assessors (aged 20–45 years, male-to-female ratio 1:1) with two years' experience in sensory analysis. Prior to participation, all panelists signed written informed consent forms confirming that they participated voluntarily, were free to withdraw from the study at any stage, and agreed that their anonymized data could be used for research purposes. The sensory evaluation standards for these honey samples (Supplementary Table S1) were developed according to Chinese standard (SN/T-2012), ISO 13299, and some other published papers with some modification[21], comprising four key attributes: color, physical state, taste, and aroma. To further refine the aroma profiling, panelists described honey aromas based solely on personal perception without preconceived lexical bias, documenting all detectable aroma attributes. Through collaborative discussion, the team eliminated subjective preference terms and redundant descriptors, consolidated synonymous terminology, and established the following eight core descriptors and their corresponding reference standards: honey-like (phenylacetaldehyde), floral (linalool), creamy (acetoin), cooling (L-menthol), woody (oak lactone), fruity (Isoamyl acetate), sweet (vanillin), and off-odor. Prior to formal evaluation, all panelists underwent a 14-d training program (1 h/d, totaling 14 h) to standardize their understanding of the scoring criteria. Sensory analyses were conducted in a controlled environment with optimal temperature (20–22 °C), uniform lighting (D65 standard), and adequate ventilation. Each honey sample was prepared in triplicate (15 g per aliquot in 30 mL transparent cups) for visual inspection, olfactory assessment, and oral tasting. All samples were coded with random three-digit numbers and presented to the panelists in a randomized order. The panelists were blinded to the treatment information during evaluation and were required to rinse their mouths with purified water between samples to minimize carry-over effects and sensory bias. Mean scores from the panelists were calculated for descriptive comparison, and the results were visualized using radar charts and bar graphs.

HS-SPME-GC-MS detection

HS-SPME conditions

Firstly, 4 g of honey, 0.1 g of NaCl, 4 mL of ultrapure water, and 10 μL of 2-octanol internal standard solution (1.00 mg/mL) were weighed into a 20 mL headspace sampling vial. Next, the sealed vial was placed on a thermostatic magnetic stirrer (60 °C, 500 r/min) for 10 min to equilibrate, and subsequently an SPME extraction fiber (50/30 μm, DVB/CAR/PDMS, Supelco, USA) was inserted into it and kept for volatile extraction (50 min) in the headspace.

GC-MS conditions

At the end of the extraction, the SPME fiber was immediately inserted into the injection port (260 °C) of the GC-MS system (QP2010, SHIMADZU, Japan) equipped with a DB-5MS column (30 m × 0.25 mm × 0.25 μm, Agilent, USA) and desorbed for 5 min. The GC parameters were set as follows: splitless injection; carrier gas: 99.999% He (1 mL/min); heating program: 40 °C for 5 min, then a gradient of 4 °C/min to 160 °C and held for 2 min, then a gradient of 10 °C/min to 230 °C and held for 5 min. The MS parameters were set as follows: transfer line temperature: 250 °C; ion source temperature: 230 °C; ionization mode: EI (70 eV); acquisition mode: scan; scanning range: 35–350 *m/z*[22].

Identification and semi-quantification of VOCs

After eliminating impurity peaks from silicone compounds derived from column bleed and SPME fiber coating detachment, Volatile organic compounds (VOCs) were selected based on ≥ 80% match. Retention indices (RIs) were determined using retention times (RTs) of C7–C40 n-alkanes mixed standards. VOC identification was achieved by comparing experimental RIs and mass spectral fragments against those in the NIST 17 (National Institute of Standards and Technology, USA) database. Semi-quantification of VOCs followed Eq. (1):

$$C_i = \frac{A_i}{A_k} \times C_k \quad (1)$$

where, C_i was the relative concentration of the target VOC (μg/g); A_i was the peak area of the target VOC; C_k was the internal standard concentration (μg/g); A_k was the internal standard peak area.

HS-GC-IMS detection

HS conditions

One gram of Honey and 5 μL of 2-methyl-3-heptanone internal standard solution (0.50 mg/mL in ultrapure water) were added to a 20 mL headspace vial. After incubation at 60 °C for 15 min with 500 r/min agitation, samples were injected using a CTC-PAL 3 static headspace autosampler (CTC Analytics AG, Switzerland) under the following conditions: splitless injection mode; injection volume: 500 μL; agitator temperature: 85 °C.

GC-IMS conditions

VOCs were analyzed using a Flavourspec® GC-IMS instrument (G.A.S., Germany) equipped with a DB-WAX capillary column (15 m × 0.53 mm × 1.0 μm, Restek, USA). GC parameters: column temperature: 60 °C; carrier gas: He (≥ 99.999%); flow program: initial flow 2.00 mL/min (hold 2 min), ramp to 10.00 mL/min over 8 min, then to 100.00 mL/min over 10 min (hold 10 min); injector temperature: 80 °C. IMS parameters: ionization source: tritium (^{3}H); drift tube length: 53 mm; electric field: 500 V/cm; drift tube temperature: 45 °C; drift gas: N_2 (≥ 99.999%); flow rate: 150 mL/min; ionization mode: positive[18].

Identification and semi-quantification of VOCs by GC-IMS

C4–C9 n-ketone mixed standard was analyzed to establish calibration curves for retention time (RT) and retention index (RI). Target compound RIs were calculated from experimental RTs and identified by matching against the VOCal software's integrated databases (NIST 2020 GC-RI library and IMS drift time database). Semi-quantification followed the identical protocol to GC-MS analysis, with 2-methyl-3-heptanone substituted as the internal standard.

Calculation of ROAVs and OCR for VOCs

The relative odor activity value (ROAV) was used to estimate the contribution of each VOC to overall flavor perception. The sources of odor thresholds are described in the note of Supplementary Table S3. For consistency, only thresholds determined in water were selected, and values reported in different units were converted to μg/g to match the semi-quantified VOC concentrations in honey. Considering that the high-sugar and high-viscosity matrix of honey may affect volatile release and sensory perception, ROAV and OCR values were used as semi-quantitative indicators for comparing the relative aroma contributions of VOCs rather than as absolute sensory impact values. The VOC with maximal flavor impact was assigned ROAV = 100. ROAVs of other compounds were calculated as Eq. (2):

$$ROAV_i = \frac{C_i}{T_i} \times \frac{T_{max}}{C_{max}} \times 100 \quad (2)$$

where, $ROAV_i$ was the relative odor activity value of the given component; C_i was the relative concentration of the given component

https://doi.org/10.48130/fia-0026-0046

(μg/g); T_i was the odor threshold of given component (μg/g); C_{max} was the relative concentration of the dominant component (μg/g); T_{max} was the odor threshold of the dominant component (μg/g). Odor contribution rate (OCR, %) for each VOC is mathematically derived from the ratio of its ROAV to the sum of all ROAVs in the sample.

Statistical analysis

All data were derived from at least three replicate experiments and expressed as mean ± standard deviation, calculated using Microsoft Excel 2010 (Microsoft, USA). Statistical analyses were performed using SPSS 26.0 software (IBM, USA) with one-way analysis of variance (ANOVA), and multiple comparison analyses were conducted via Duncan's test and unpaired *t*-test to assess significant differences ($p \leq 0.05$). The 3D spectra, 2D spectra, difference spectra, and fingerprints of volatile components based on GC-IMS were generated using plugins such as Reporter, Gallery Plot, and Dynamic in the VOCal software. Venn diagrams and bar charts were plotted using Origin 2022 (OriginLab, USA). Upset plots, clustering heatmaps, and PCA were visualized using tools provided by ChiPlot (www.chiplot.online). The chemical structures of compounds were drawn using ChemDraw 22.2.0 (PerkinElmer, USA).

Results and discussion

Nectar-source identification by melissopalynology

The morphological characteristics and relative abundance of pollen grains in honey serve as key indicators for identifying botanical origins, and the samples containing > 45% dominant pollen can be classified as unifloral honey[22]. The SEM images captured from the honey samples collected in April (Supplementary Fig. S1c, S1d) either in low- or high-altitude areas (HMH and LMH) showed varieties of pollen with no predominant occupation, suggesting HMH and LMH were both multisource honeys. The March-collected samples displayed large quantities of pollen with spherical or subspherical equatorial views, trilete circular polar views, three germination furrows, and coarse reticulate striations on the exine surface (Supplementary Fig. S1b), showing the pollen frequency at 72.71% ± 2.09%, representing *Brassica chinensis* L. as the main nectar source[23]. Then, the August-collected samples exhibited predominant pollen (59.32% ± 4.47%) with ovate equatorial views, subcircular polar views with three narrow-elongate germinal furrows, and an exine surface bearing irregular striate ornamentation (Supplementary Fig. S1a), suggesting the samples were GH with *Rhus chinensis* Mill. as the main nectar source[22].

Microbial loads in freshly collected honey samples

With no detection of the common pathogenic bacteria, including coliforms, *Salmonella*, *Shigella*, *Staphylococcus aureus*, in any of the fresh-collected honey samples (Supplementary Table S4), the total plate counts (TPC) for aerobic bacteria in LMH, HMH, RH, and GH ranged from 59.68 ± 5.34 to 160.00 ± 40.00 CFU/g, while the mold counts varied between 36.72 ± 4.38 and 55.47 ± 6.15 CFU/g. Osmophilic yeast levels spanned 61.65 ± 7.21 to 116.67 ± 15.28 CFU/g. Notably, likely attributable to the elevated seasonal temperatures during collection that favored microbial proliferation[24], GH samples exhibited the most pronounced microbial contamination among all the honey samples collected in the Fengtong area, which were taken for further experiments with irradiation sterilization treatment (IST) and VCT.

Decontamination efficiency of γ-irradiation in GH

After 10 d of cultivation at 37 °C, the TPC of the aerobic bacteria, mold, and osmophilic yeasts in the control group (without any microbial control treatment) were assayed to be 2,273.33 ± 193.15 CFU/g, 373.33 ± 23.63 CFU/g and 1,200 ± 103.32 CFU/g, respectively, showing an over 14-fold, 8-fold and 10-fold multiplication compared with the pre-storage samples (Fig. 1a, c, d), and coliform bacteria were even detected at 6.67 ± 2.89 CFU/g in control after 10 d of cultivation (Fig. 1b), suggesting the relatively higher microbiological risks in GH than the other samples collected at lower air temperature during storage.

Besides, the post-storage VCT samples showed a slight increase in aerobic bacteria and osmophilic yeasts TPCs to 376.67 ± 71.12 CFU/g and 196.67 ± 15.28 CFU/g, respectively, with faster growth of mold to 186.67 ± 18.93 CFU/g (Fig. 1a, c, d). For the samples with IST, aerobic bacteria, molds, and osmophilic yeasts were virtually undetectable in IS6-0 and IS8-0, while those in IS4-0 were counted to be 60 CFU/g, 6.67 CFU/g, and 30 CFU/g, respectively. Compared to pre-storage samples, the aerobic bacteria, molds, and osmophilic yeasts in IS4-10 increased to 446.67 CFU/g, 210.00 CFU/g, and 280.00 CFU/g respectively, exceeding Chinese National Standard Limits (≤ 200 CFU/g) for both mold and osmophilic yeast counts, whereas those in IS8-10 showed significantly lower levels at 83.33 CFU/g, 23.33 CFU/g, and 23.33 CFU/g (Fig. 1a, c, d). These results demonstrated that VCT partly inhibited aerobic bacterial growth but was insufficient for fungal control, while IST showed an efficient sterilization effect at 8 kGy with no significant microbial proliferation even after 10 d of accelerated storage.

Changes in microbial composition

Bacterial community composition

The sequencing metrics obtained from 16S rRNA amplicon sequencing, including raw reads, filtered reads, denoised reads, the number of ASVs, and the per-sample sequencing depth after rarefaction, are presented in Supplementary Table S5. The rarefaction curves reached a plateau, and the coverage values reached 100% (Supplementary Fig. S2a, S2e), indicating that the sequencing depth was sufficient to capture the major microbial diversity in the samples. The increase of Chao1 and Shannon indices in GH-10, VCT-10, IST-0 and IST-10 (Supplementary Table S6), combined with the results of plate colony counting (Fig. 1a–d), suggests the probable multiplication of low-abundance bacteria during storage, as well as the reduction of dominant bacteria after γ-irradiation. PCA analysis (Supplementary Fig. S2b–S2d) at the phylum, genus, or species levels showed inter-group dispersion and within-group clustering, with the summary of PC1 and PC2 over 70%, while the distance between the groups demonstrated that, compared with the distinct effect of storage, diverse pretreatment caused more significant differences in bacterial composition among different groups.

Bacillota (*Firmicutes*) and *Pseudomonadota* were predominant (> 2%) bacteria phylum in GH-0, occupying 55.34% and 44.29% (Supplementary Fig. S2i), respectively corresponding to the dominant genus *Apilactobacillus* and *Bombella*, with the proportions at 50.85% and 39.91% (Fig. 1e). *Apilactobacillus* was a commonly found lactic acid bacterium (LAB) in bees and flowers[25], while *Bombella* was an acetic acid bacterium that colonized in honeybee intestines, being beneficial to resisting fungal pathogens[26]. After 10 d of accelerated storage in GH-10, besides *Bacillota* (53.38%) and

https://doi.org/10.48130/fia-0026-0046

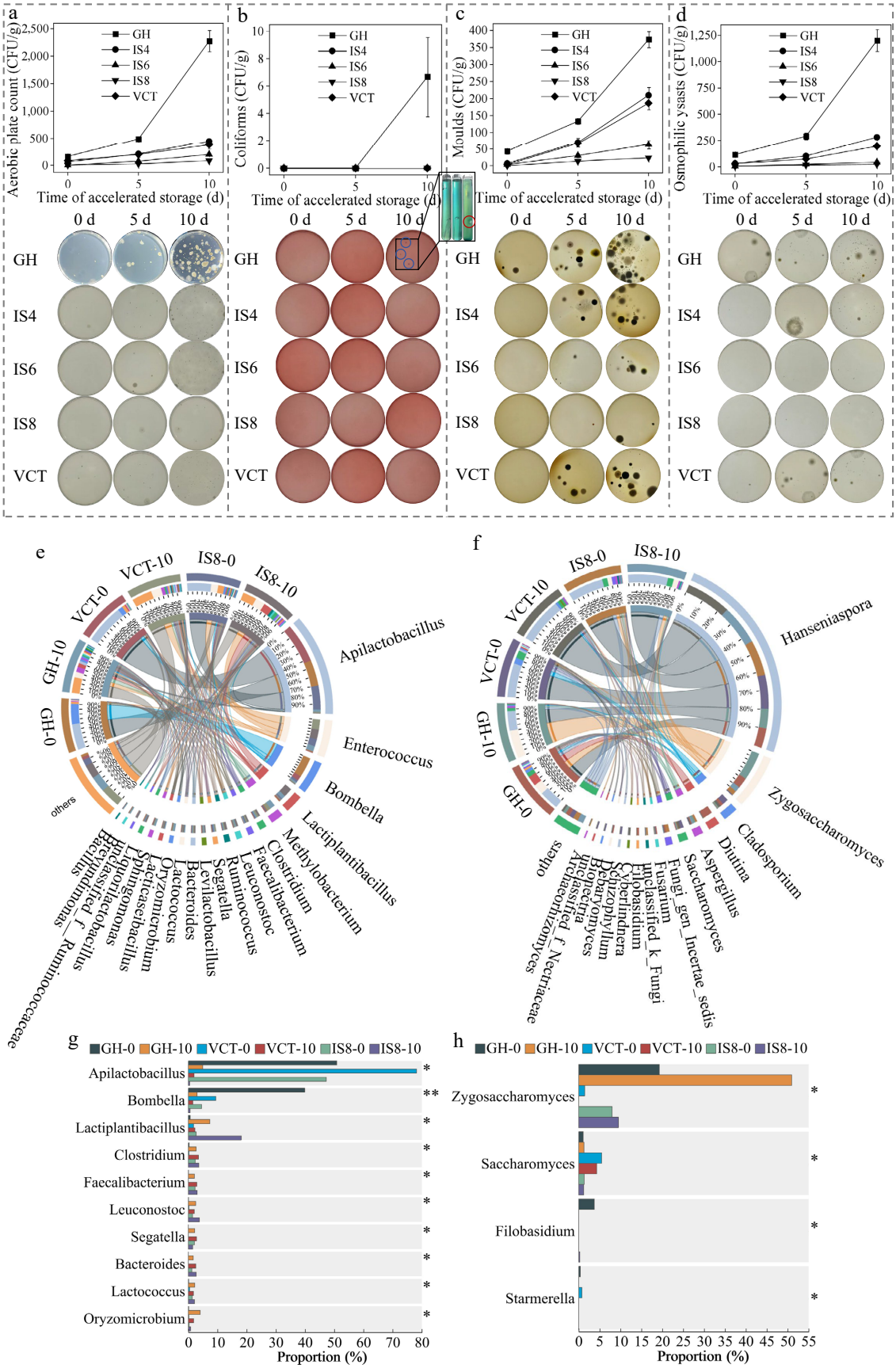

Fig. 1 Influence of different preservation strategies on microbial multiplication and composition. Total colony numbers of (a) aerobic microbes, (b) coliforms, (c) molds, and (d) osmophilic yeasts. (e) Circos plot of fungal community and (f) bacterial community at the genus level. Intergroup differential genera of (g) bacteria and (h) fungi.

https://doi.org/10.48130/fia-0026-0046

Pseudomonadota (37.26%), *Bacteroidota* arose to be a dominant phylum (4.47%). Surprisingly, *Enterococcus* surpassed all the other genera and became predominant with 10.97% proportion, sequentially followed by *Methylobacterium* (10.38%), *Lactiplantibacillus* (7.36%), *Apilactobacillus* (4.92%), *Oryzomicrobium* (4.06%), *Sphingomonas* (3.2%), and *Bombella* (3.00%), as well as *Clostridium*, *Faecalibacterium*, *Leuconostoc*, *Segatella*, *Levilactobacillus*, *Lactococcus*, *Lacticaseibacillus*, *Brevundimonas*, and *Bacillus*, occupying no more than 2.7% of each (Fig. 1e, g). These findings suggested that the initial dominant bacteria originated from honeybees and pollen grew slowly. In addition to the multiplication of probiotic bacteria, such as *Lactiplantibacillus*, *Leuconostoc*, *Lactococcus*, and *Lacticaseibacillus*[27], the increased relative abundances of genus-level *Enterococcus, Faecalibacterium*, *Clostridium*[28], and *Methylobacterium*[29] indicated microbial community shifts in GH honey during its shelf-life, although these genera showed extremely low contents initially. Since these taxa were identified only at the genus level, they were interpreted as potentially undesirable or opportunistic taxa rather than direct evidence of pathogenic bacteria.

A similar bacterial community was detected in VCT-0 and even in VCT-10 after accelerated storage, except for a decrease in *Pseudomonadota* to 14.85% (Supplementary Fig. S2i). However, compared to GH-10, VCT-10 showed higher proportions of *Enterococcus* (20.2%), *Clostridium* (3.48%), and *Faecalibacterium* (2.90%), but a lower proportion of *Lactiplantibacillus* (2.25%, Fig. 1e, g). This result suggested that VCT partly inhibited bacterial growth in GH, but there was still a high risk of *Enterococcus*, *Clostridium*, and *Faecalibacterium* multiplication. Notably, the detection and increased relative abundance of *Clostridium* deserve particular attention, as clostridial spores are highly resistant to adverse environmental conditions and may survive dehydration-based treatments[30]. Once favorable conditions are encountered during subsequent storage, dilution, or processing of honey-containing products, these spores may germinate and develop into vegetative cells, thereby increasing potential food safety risks.

IST (8 kGy) caused an immediate change in the bacterial community, leading to a significant decrease in *Pseudomonadota* (9.65%), and an indirect increase in the proportions of *Bacillota* (85.03%) and *Bacteroidota* (3.47%, Supplementary Fig. S2i). *Apilactobacillus* (47.26%) and *Enterococcus* (13.95%), which belong to *Bacillota*, became the main dominant genera, followed by *Bombella*, *Lactiplantibacillus*, *Clostridium, Faecalibacterium*, and *Segatella* (Fig. 1e, g). After storage, *Apilactobacillus* and *Bombella* decreased to 0.45% and 0.60%, respectively, and *Enterococcus* and *Lactiplantibacillus* became dominant at 19.20% and 18.16%. These findings suggested the different sensitivity of GH-originated bacteria to γ-irradiation, *Pseudomonadota*, as well as *Apilactobacillus* and *Bombella*, was sensitive to γ-irradiation or post-irradiation bactericidal effect, while *Lactiplantibacillus* and *Enterococcus* were more resistant.

Fungal community composition

The sequencing metrics obtained from ITS amplicon sequencing, including raw reads, filtered reads, denoised reads, the number of ASVs, and the per-sample sequencing depth after rarefaction, are presented in Supplementary Table S5. Storage showed no significant influence on Chao and Shannon indices in fungal community composition, and VCT induced an immediate decrease in the alpha diversity of GH, which rebounded after storage, while IST at 8 kGy caused both an immediate and post-storage increase in Chao1 and a decrease in Shannon indices (Supplementary Table S6). PCA analysis at the phylum level showed the location of GH-0 at positive *X*-axis together with GH-10, while the VCT samples were in the third quadrant and IS8 samples in the fourth quadrant, suggesting significant intergroup differences, similar to bacterial community compositions (Supplementary Fig. S2g).

28 Fungal species and 25 genera belonging to five phyla were identified here (Supplementary Fig. S2l–S2n). *Ascomycota* was detected to be predominant in GH-0 occupying 88.88%, followed by *Basidiomycota* 7.33%, showing *Hanseniaspora thailandica* (35.40%), *Diutina catenulata* (18.12%), *Zygosaccharomyces siamensis* (17.50%), *Filobasidium* sp. (3.72%), an unclassified *Debaryomyces* and an unclassified *Cladosporium* (5.35%) as dominant fungal species (Fig. 1f, h; Supplementary Fig. S2l–S2n). *H. thailandica* is a common fungus in honey, natural fermentation environment and on fruit surface, producing aromatic esters[31]. *Zygosaccharomyces* was considered the main source causing spoilage of juice, honey, soy sauce, and sauces, showing strong resistance to high sugar contents and high osmotic pressure[32], and *Debaryomyces* was reported to be a common fungus inducing food spoilage[33], while *Diutina catenulata* and *Filobasidium sp.* were opportunistic pathogens. After 10 d of storage, dominant fungal species changed to *Z. siamensis*, *H. thailandica*, *Zygosaccharomyces mellis*, *Aspergillus spiculosus*, and an unclassified *Cladosporium*, with the proportions of 46.64%, 35.82%, 3.73%, 2.91%, and 2.13% (Fig. 1f, h), respectively. This finding suggested that yeasts, especially *H. thailandica* and *Z. siamensis*, dominated the fungal community composition in fresh-collected GH honey, which were the main sources resulting in GH spoilage, as well as the growth of *A. spiculosus*.

VCT caused immediate increase of *Ascomycota* proportion, along with the reduction of *Zygosaccharomyces* (Supplementary Fig. S2l–S2n). *H. thailandica* and an unclassified *Cladosporium* were found to be dominant *species at* 61.60% and 10.97%, respectively, followed by *Saccharomyces* sp., an unclassified *Schizophyllum*, *Bionectria solani*, and unclassified *Nectriaceae*, and after storage, the proportion of *H. thailandica* further increased to 81.85% (Fig. 1f, h; Supplementary Fig. S2l–S2n). This finding suggested that VCT could reduce the proportion of *Zygosaccharomyces*, *Diutina*, and *Filobasidium* in GH, and *H. thailandica* became the main fungal risk of GH spoilage during VCT sample storage.

In IST-0 (8 kGy), the dominant fungal phyla were *Ascomycota* (84.55%) and *Mortierellomycota* (3.88%), with *H. thailandica*, *Z. siamensis*, *A. spiculosus*, and *Archaeorhizomyces* sp. as dominant species, occupying 64.49%, 7.64%, 6.26%, and 2.05%, respectively (Fig. 1f, h; Supplementary Fig. S2l–S2n). After 10 d of storage, dominant phyla changed to *Ascomycota* (94.55%) and *Basidiomycota* (3.03%), while *A. spiculosus* and *Archaeorhizomyces* sp. decreased to less than 1%. These results demonstrated that besides the general sensitivity to γ-irradiation or its post-bactericidal effect, *Hanseniaspora* could be more resistant than *Zygosaccharomyces*, *Archaeorhizomyces*, *Aspergillus*, *Diutina*, and *Filobasidium*.

In summary, the microbial community composition changes suggested that the fresh-collected GH samples contained diverse fungi, and with honeybee- and pollen-originating probiotics as primary bacteria, such as *Apilactobacillus* and *Bombella*. However, the growth of spoilage-associated taxa during storage, including *Enterococcus*, *Faecalibacterium*, *Clostridium*, and *Methylobacterium*, as well as osmotolerant yeasts, mainly *Hanseniaspora* and *Zygosaccharomyces*, led to the risk of honey spoilage, which could not be controlled by regular dehydration treatment such as VCT. Nevertheless, γ-irradiation at 8 kGy exhibited remarkable sterilization effect in GH and almost inhibited the growth of all the strains, although the higher resistance of *Lactiplantibacillus*, *Enterococcus* and *Hanseniaspora* was still worthy of attention.

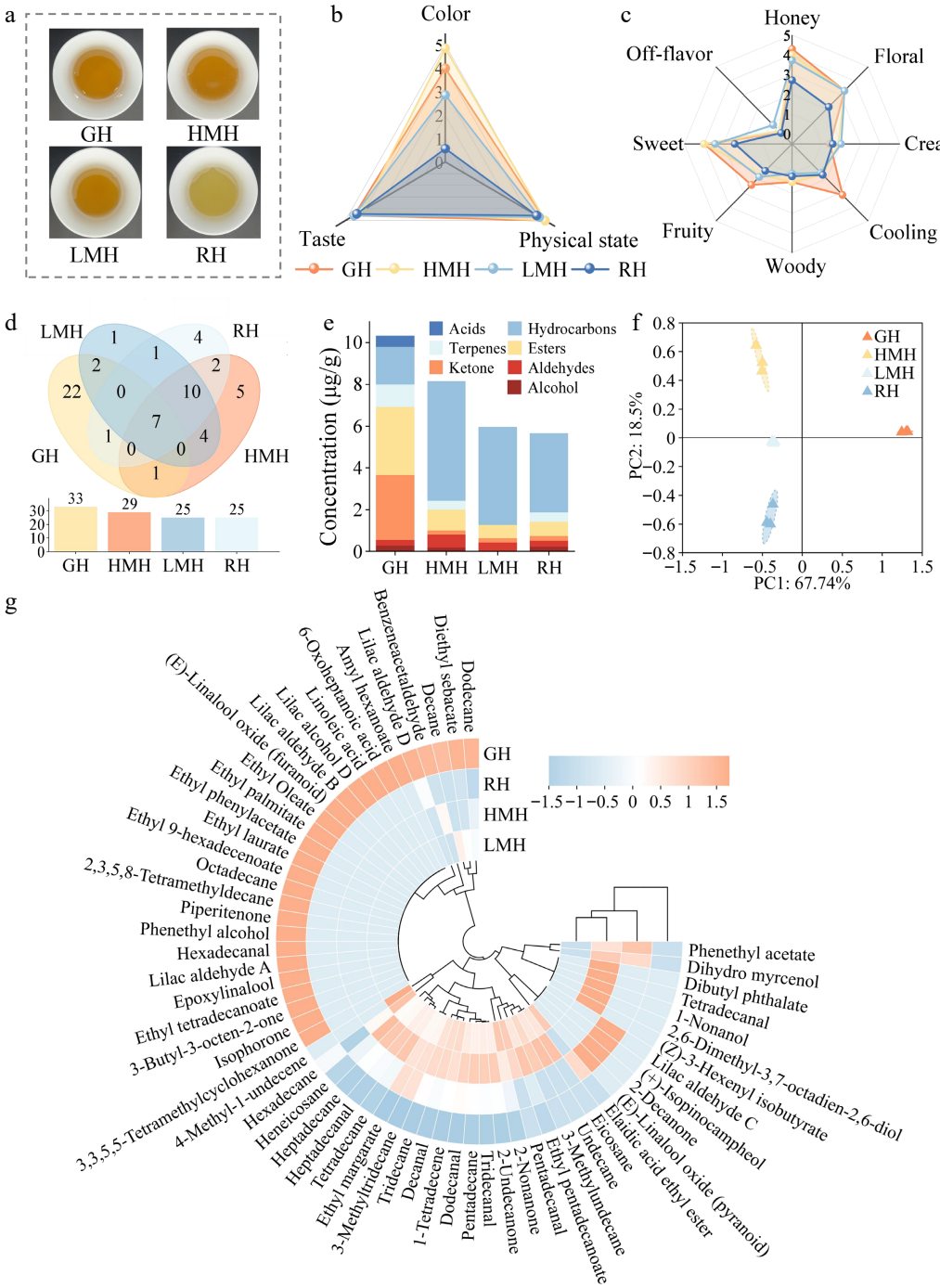

Fig. 2 Sensory evaluation and GC-MS detected VOC composition of GH, HMH, LMH, and RH. (a) Color and appearance. (b) Color, taste, and physical state scores. (c) Flavor scores. (d) Venn diagram of VOCs. (e) Concentration of different classes of VOCs. (f) PCA score plot. (g) Hierarchical clustering heatmap of the VOCs.

Changes in the sensory quality of GH under different treatments during storage

Sensory properties of freshly collected GH

Except for the water-white color of RH, all the honey samples had an amber and viscous appearance (Fig. 2a, b), showing similar sweet and smooth tastes. Referring to olfactory flavors, eight dimensions were reported in sensory evaluation with no off-flavor in each sample, and GH showed its unique flavor in stronger fragrances (scores > 3.0) of honey, floral, cooling, fruity, and sweet, with subtle aroma of woody and creamy (scores < 2.0; Fig. 2c).

Changes in the sensory properties of GH after storage

Sensory evaluation suggested no significant change in fluid state (scores > 4.0) in each sample after storage (Fig. 3a, b; Supplementary Fig. S3b). IST induced color fading of GH, which was reversed after accelerated storage (Fig. 3a, b; Supplementary Fig. S3a). Besides slightly weakening the honey tastes in VCT and IST samples, these two kinds of pretreatment produced different effects on olfactory flavors (Supplementary Fig. S3c). VCT caused an immediate decrease in floral, cooling, fruity, and sweet odors in GH (Fig. 3a;

https://doi.org/10.48130/fia-0026-0046

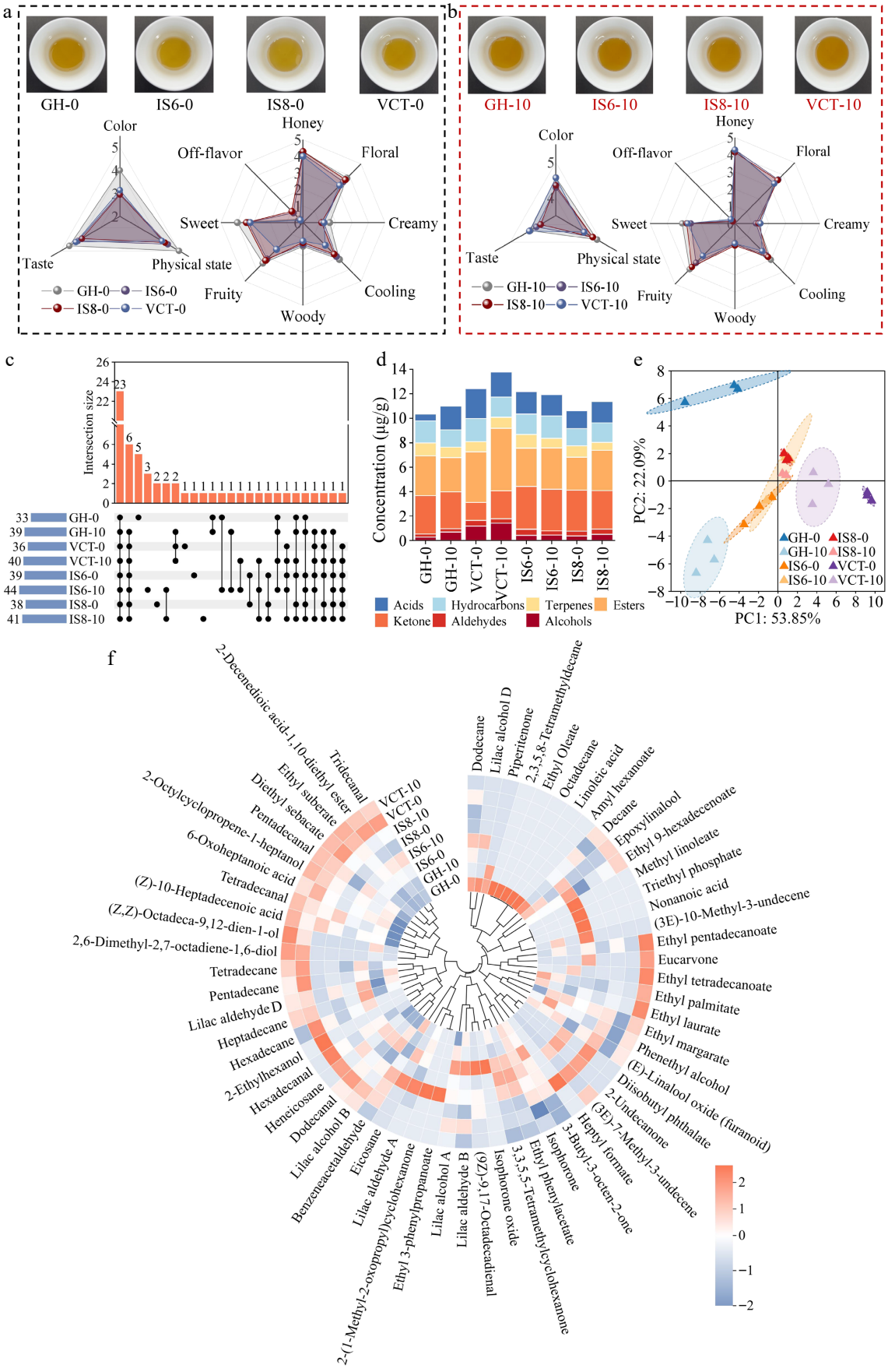

Fig. 3 Sensory evaluation and VOC composition changes of GH after different preservation treatments. Appearance and scores radar plot: (a) before and (b) after storage. (c) Up-set plot of VOCs, (d) concentration of different classes of VOCs, (e) PCA score plot, (f) hierarchical clustering heatmap of VOCs.

Supplementary Fig. S3e, S3g, S3i, S3j), while IST showed no immediate influence on GH original flavors, but generated a slight oxidizing odor (score: 0.86–0.93, Supplementary Fig. S3d–S3k). After storage, the sweet fragrances decreased in each sample; however, the oxidizing odor in IST samples also disappeared (Fig. 3a, b; Supplementary Fig. S3j, S3k). This result suggested that 6–8 kGy IST had no significant influence on the sensory quality of the post-storage GH samples, and compared with VCT, IST better retained the GH characteristic aroma.

Changes in flavor substances detected by GC-MS

Identification of critical flavor substances

A total of 60 VOCs were identified in the four honey samples, including four alcohols, eight aldehydes, six ketones, 14 esters, ten terpenes, 16 hydrocarbons, and two acids (Supplementary Table S7), respectively. The composition of VOCs in different samples is significantly distinct (Fig. 2d, e, g). PCA for these raw honey samples showed the aggregation within groups and separation among different groups, exhibiting the values of PC1 and PC2 at 62.64% and 19.65%, respectively (Fig. 2f). GH samples gathered in the first quadrant, staying away from the other samples in both two directions, suggesting its uniqueness in GC-MS detected VOCs, mainly due to the high contents of esters (3.26 μg/g) and ketones (3.12 μg/g, Supplementary Table S7), especially isophorone (2.66 μg/g) and ethyl palmitate (2.19 μg/g), as well as the acids 6-oxoheptanoic acid. According to ROAV calculation, 17 aroma substances of GH detected by GC-MS were identified (Supplementary Table S3). Ten of these VOCs were found to be important flavor substances (ROAV > 1.00) in GH, including three common VOCs existing in other honey samples, that is benzeneacetaldehyde (ROAV: 100, OCR: 58.99%; floral, hyacinth), dodecanal (ROAV: 6.10, OCR: 3.60%; fruity, citrus, sweet), and lilac aldehyde D (ROAV: 3.43, OCR: 2.02%; floral lilac), as well as seven GH-specific VOCs, containing isophorone (ROAV: 39.93, OCR: 23.56%; cooling, mint), phenethyl alcohol (ROAV: 1.44, OCR: 0.85%; floral, rose), ethyl phenylacetate (ROAV: 4.39, OCR: 2.59%; honey, sweet, floral, rose), ethyl tetradecanoate (ROAV: 4.25, OCR: 2.51%; beewax, sweet, floral, iris), ethyl palmitate (ROAV: 3.30, OCR: 1.95%; creamy, fruity), (E)-linalool oxide (furanoid) (ROAV: 1.45, OCR: 0.86%; woody, floral) and lilac aldehyde B (ROAV: 2.88, OCR: 1.70%; floral, lilac).

Effects of IST, VCT and storage on GC-MS detected VOCs

Sixty-one VOCs were identified in GH, VCT/IST groups and their post-storage variants, comprising five alcohols, seven aldehydes, nine ketones, 17 esters, eight terpenes, 13 hydrocarbons, and four acids by GC-MS (Supplementary Table S8). The volatile profiles differed among the honey samples in terms of the number and abundance of constituents (Fig. 3c, d, f). PCA showed aggregation within groups and separation among different groups, with the values of PC1 and PC2 at 53.85% and 22.09% (Fig. 3e), suggesting the significant differences between post-storage GH samples (GH-10), IST samples (IST-0, IST-10), VCT samples (VCT-0, VCT-10), and raw GH (GH-0). Notably, the separation magnitudes of IST samples from the control were smaller than those of VCT samples, and IS6 and IS8 groups remained statistically indistinguishable before and after storage, suggesting that 6 and 8 kGy IST produced non-significant differential effects on GH VOCs even after storage, and VCT unexpectedly exerted a greater impact on GH VOCs composition, in accordance with the sensory evaluations.

Specifically, accelerated storage (GH-10) but no other treatment caused a decrease in esters, fatty acids, and hydrocarbons in GH, with an increase in alcohols, and over 3-fold accumulation of 6-oxoheptanoic acid from 0.52 μg/g to 1.91 μg/g (Supplementary Table S8; Fig. 3d, f). The increase of alcohols due to phenethyl alcohol (to 0.37 μg/g), 2-octylcyclopropene-1-heptanol (0.21 μg/g), and 2,6-dimethyl-2,7-octadiene-1,6-diol (0.07 μg/g) as linalool derivative with a slight fatty note, showed little positive effect on aroma, while the decrease of ethyl palmitate from 2.19 μg/g to 1.77 μg/g caused the fading of creamy aroma. As previous reports, ethyl palmitate decline could be linked to autoxidative hydrolysis during honey storage, while phenethyl alcohol might also be released by phenethyl alcohol-containing glycoside through enzymatic or hydrolysis reaction during honey storage[34]. Generation of 2-octylcyclopropene-1-heptanol, corresponding to the decline of linoleic acid in GH, and the high contents of 6-oxoheptanoic acid could be attributed to microbial metabolism, insect-derived enzymatic activity, or oxidative processes, which brought in rancid off-odors and other sensory defects at elevated concentrations[35,36].

VCT induced immediate loss of some GH-specific flavor-contributing VOCs, including isophorone (down to 1.40 μg/g), ethyl palmitate, phenethyl alcohol, epoxylinalool, (E)-linalool oxide (furanoid), and 3-butyl-3-octen-2-one, resulting in the weakening of floral, woody, creamy, and especially the cooling aroma (Supplementary Table S8; Fig. 3f). However, the fruity, woody and creamy odors could be complemented during storage because the rebound of ethyl palmitate, as well as accumulation of aldehydes and esters, mainly including dodecanal, tridecanal, tetradecanal, pentadecanal, diethyl sebacate, ethyl suberate, and 2-decenedioic acid-1,10-diethyl ester. Unexpectedly, VCT samples showed the highest concentrations of the VOCs with rancid off-odors and a fatty note after storage, including 6-oxoheptanoic acid (2.44 μg/g), 2-octylcyclopropene-1-heptanol, (0.25 μg/g), and 2,6-dimethyl-2,7-octadiene-1,6-diol (0.65 μg/g), compared with the other post-storage samples. These findings suggested that VCT caused the immediate escape of flavor substances with higher volatility during the decompression process and could generate VOCs possibly associated with fatty acid oxidation and enzymatic bioconversion in honey, probably due to continuous heating with inefficient control of microorganisms.

Interestingly, γ-irradiation retained the concentration of GH-characteristic flavor substances, the relatively high contents of phenethyl alcohol, isophorone, and (E)-linalool oxide (furanoid) even after storage maintained the floral, woody and cooling aroma in GH (Supplementary Table S8; Fig. 3f). Besides, after the storage, IST samples (IS8) showed the lowest undesirable VOCs contents of 6-oxoheptanoic acid (1.43~1.69 μg/g), 2-octylcyclopropene-1-heptanol (0.14~0.19 μg/g), and 2,6-dimethyl-2,7-octadiene-1,6-diol (0 μg/g), suggesting that γ-irradiation may inactivated the microbial or *Apis cerana* enzymes needed for some specific biotransformation[37]. However, IST induced the production of some newly generated compounds at 8 kGy and caused the disappearing of epoxylinalool. (9Z)-9,17-Octadecadienal, isophorone oxide, 2-(1-methyl-2-oxopropyl)-cyclohexanone, ethyl 3-phenylpropanoate and eicosane were detected immediately after irradiation, while 2-undecanone, eucarvone, triethyl phosphate, heptyl formate, di-isobutyl phthalate linoleic acid methyl ester, (3E)-10-methyl-3-undecene, and nonanoic acid appeared after storage, suggesting that with the protection of original flavor substances and preventing rancid off-odors, γ-irradiation may initiate the lipid peroxidation- and Maillard-related pathway while inducing cleavage and rearrangement of specific chemical structures, thereby giving rise to newly formed esters, hydrocarbons, oxidized compounds, and other derivatives.

https://doi.org/10.48130/fia-0026-0046

HS-GC-IMS detection for VOCs

VOCs identification and critical flavor substances screening

HS-GC-IMS were employed to further elucidate the flavor substances change during storage, VCT and IST, and 69 VOCs were detected (Fig. 4b) with 55 definitively identified through database alignment (Supplementary Table S9), and 40 distinct compounds were remained considering the monomeric and dimeric forms produced in high concentrations or strong intermolecular interactions during ionization, including 11 alcohols, seven aldehydes, nine ketones, six esters, two terpenes, one acid, three furans, and one sulfur-containing compound (Fig. 4d). The ROAVs and OCRs of the compounds were calculated according to odor thresholds (Supplementary Table S3), and seven compounds with ROAV > 1 were established as key flavor contributors in GH: 1-hexanol (ROAV: 1.78, OCR: 1.31%; fruity, foiage, woody), 3-methyl-1-butanol (ROAV: 1.81, OCR: 1.33%; fruity, apple), (E,E)-2,4-octadienal (ROAV: 15.93, OCR: 11.72%; fruity, pear), 1-nonanal (ROAV: 7.41, OCR: 5.45%; floral, fruity, citrus), heptaldehyde (ROAV: 4.83, OCR: 3.55%; ruity, pungent), 3-hydroxy-2-butanone (ROAV: 1.98, OCR: 1.46%; creamy), and ethyl isovalerate (ROAV: 100, OCR: 73.57%; fruity, apple), which complement the characteristic VOCs identified by GC-MS that contributed the key aroma of GH, especially in fruity and creamy (Fig. 5).

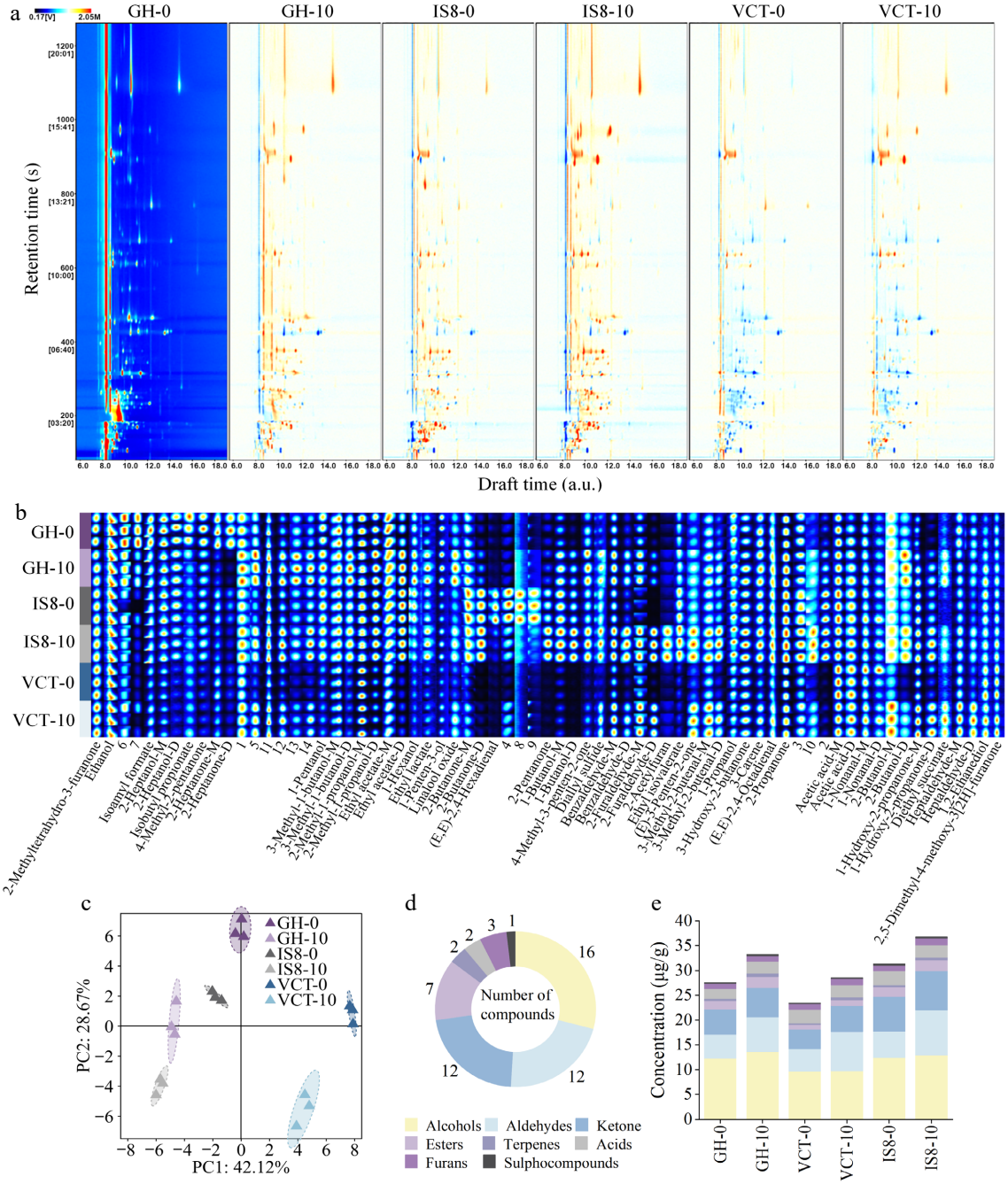

Fig. 4 GC-IMS-detected VOCs composition changes of GH after different preservation treatments. (a) Volatile difference plot, (b) volatile fingerprints, (c) PCA score plot, (d) number of VOCs, (e) concentration of different classes of VOCs.

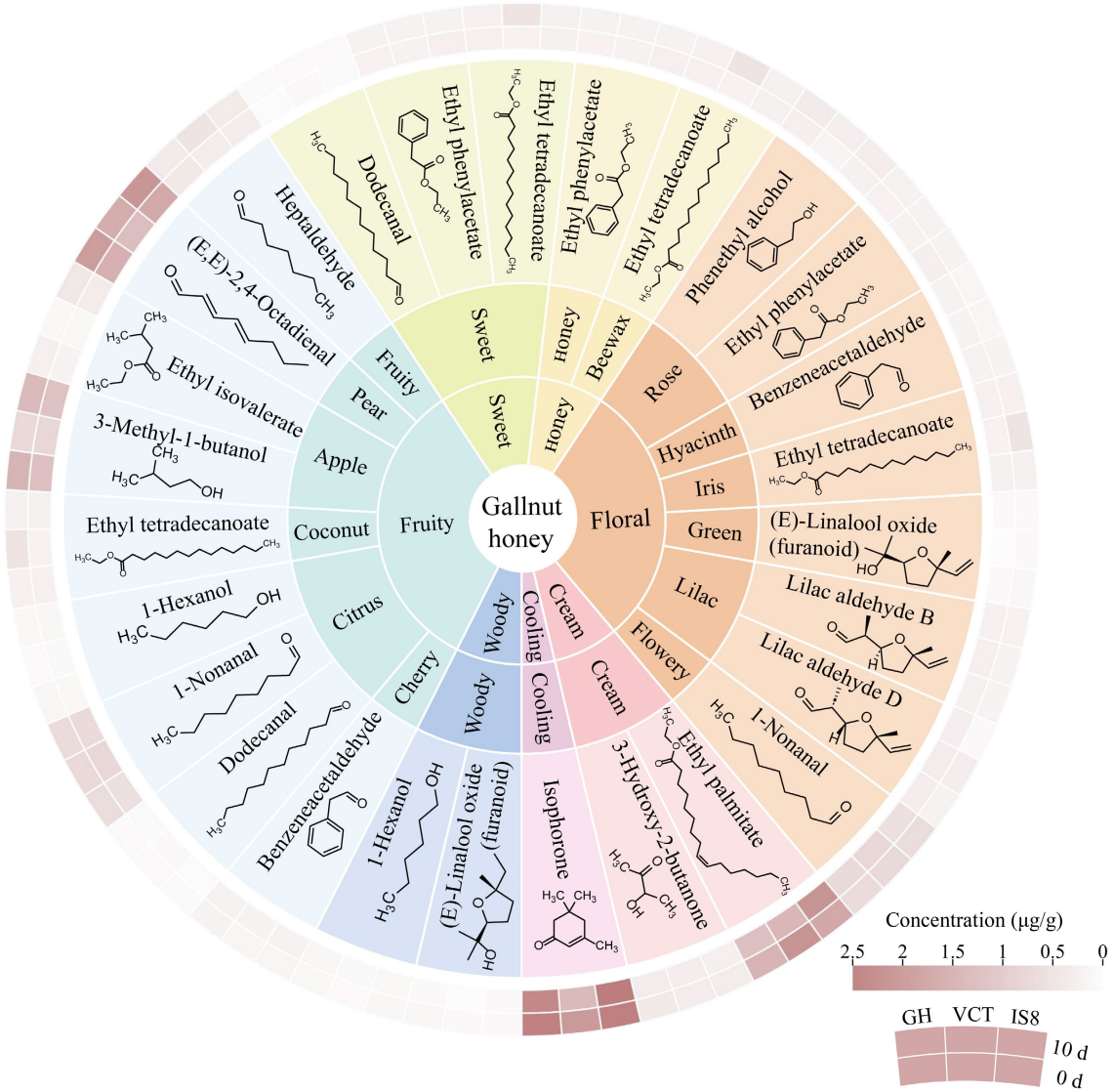

Fig. 5 Key aroma and aroma substances change in GH caused by different preservation treatments. Level 1: Odor descriptors; Level 2: Idiographic odor characteristics; Level 3: Corresponding volatile compounds with structures; Perimeter heatmap: Concentration changes across treatments and storage.

Effects of IST, VCT and storage on GC-IMS detected VOCs

The ion signals of GH samples distributed in the scope from 1.0 a.u. to 1.6 a.u. in *X*-axis with 200–1,200 s in *Y*-axis, showing overall similarity but local specificity (Supplementary Fig. S4). PCA based on VOCs peak areas (Fig. 4c) showed distinct intra-group clustering and inter-group dispersion, with PC1 and PC2 collectively accounting for 70.79% of total variance, suggesting significant and similar VOCs composition variation after storage, with storage trajectories parallel to GH both in IST- and VCT groups. Notably, the closer proximity of IST groups to GH vs VCT groups signified comparatively milder VOC modifications by IST, being consistent with PCA results in GC-MS detection.

Storage induced an overall VOCs increase (Fig. 4b, e; Supplementary Table S9). The elevated concentration of acetic acid, alcohols (3-methyl-1-butanol, 1-butanol, 2-methyl-1-propanol, and ethanol), esters (diethyl succinate, ethyl lactate, ethyl isovalerate, and ethyl acetate), and diallyl sulfide (from 0.20 μg/g to 0.36 μg/g), represents microbial activities related to alcohol metabolism, esterification, and sulfur-containing precursors degradation[34], while the increase of linalool oxide and 3-carene indicating the lively biochemical reactions. Furthermore, the detection of 2-furaldehyde, as an indicator representing honey freshness which generated from enolization and β-elimination of pentose and hexose[38], high levels of 2-acetylfuran, as a glucose degradation product through the reaction of glucose's C-5 unit with the methyl in amino acids[39], and (E, E)-2, 4-octadienal as oxidative degradation product of the lipid[40], as well as benzaldehyde, 2-butanone, 2-propanone, and 1-hydroxy-2-propanone, which were usually generated by Strecker degradation and Maillard reaction[41], all suggested that the decreased freshness in GH during storage.

The lowest VOCs contents in VCT-0 suggested the overall loss of flavor substances immediately after VCT (Fig. 4a, b, e), showing the general decline in GH-original alcohols, ketones, and esters (Fig. 4e), including 2-heptanol, 1-pentanol, 3-methyl-1-butanol, 2-methyl-1-propanol, 1-propanol, ethanol, 2-butanone, 2-propanone, 4-methyl-2-pentanone, 2-heptanone, ethyl isovalerate, ethyl acetate and isoamyl formate. But acetic acid, 2,5-dimethyl-4-methoxy-3[2H]-furanone, and 2-methyltetrahydro-3-furanone, which could bring in fermentation and nut-burnt aroma into GH, were significantly

https://doi.org/10.48130/fia-0026-0046

increased after VCT. This means that VCT may accelerate the Maillard and fermentation-related reaction processes. Furthermore, in contrast to GH-10, VCT slowed down the accumulation of esters during storage, however, some other storage degradation products significantly increased, including 1-hydroxy-2-propanone, 2-furaldehyde, benzaldehyde and (E, E) -2,4-octadienal, which could further

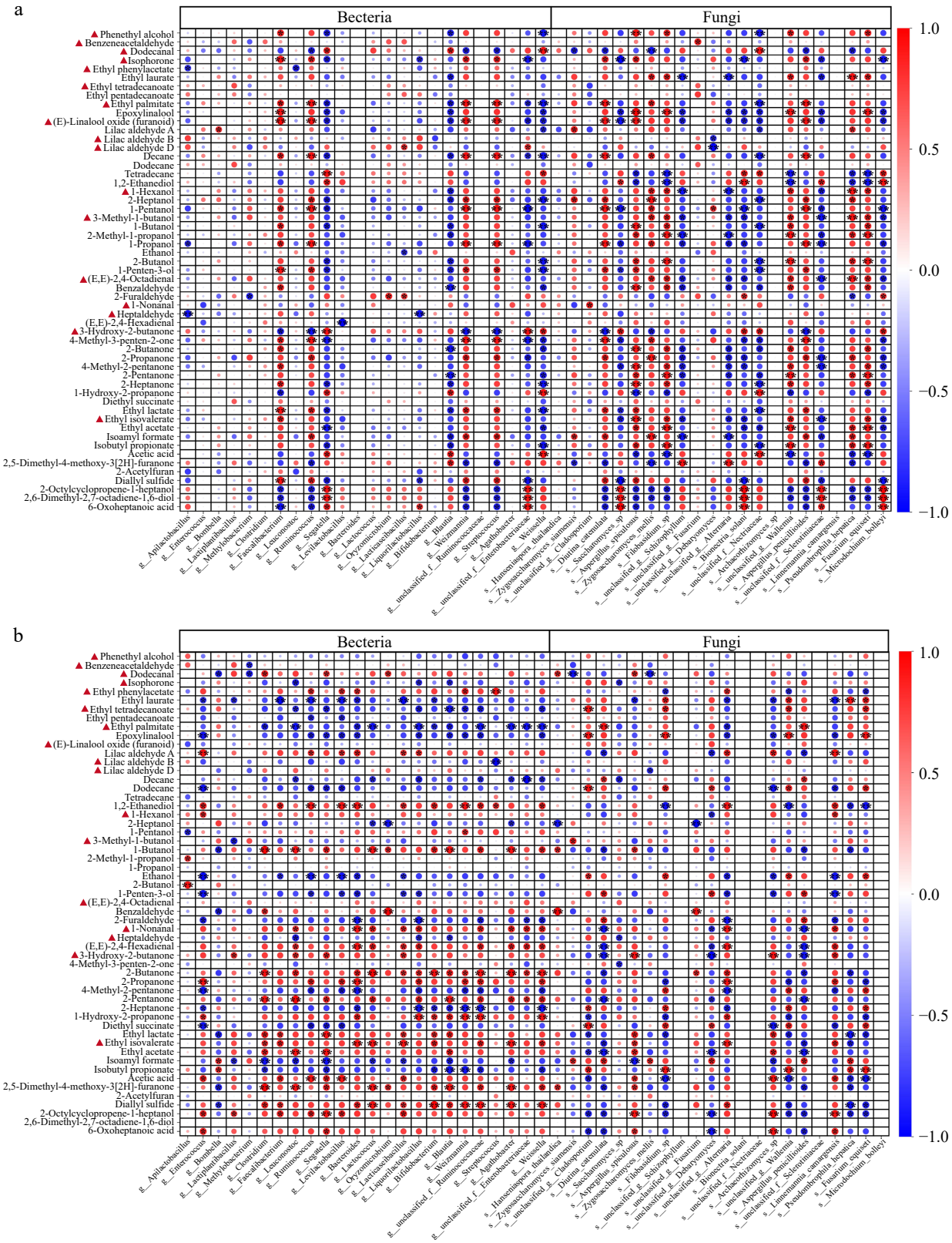

Note: '▲' indicates volatile compounds with ROAV > 1. '**' indicates $0.8 < |R| < 0.9$, and '***' indicates $|R| > 0.9$.

Fig. 6 Correlation heatmap between microorganisms and VOCs in vacuum-concentrated and γ-irradiated honey samples. (a) Vacuum concentration group. (b) 8 kGy γ-irradiation group.

enhance the nut-burnt aroma in GH. This result suggested VCT did not abort the ongoing microbial activity and biochemical reactions happened in storage, but also induced direct depletion of GH-specific VOCs.

IST samples showed the most VOCs abundant (Fig. 4a, b, e), causing an increase of esters, including ethyl acetate, and ethyl isovalerate, as well as ketones, particularly containing 2-butanone, 2-propanone, and 1-hydroxy-2-propanone immediately after 8 kGy γ-irradiation, with a minor reductions in diethyl succinate, isoamyl formate, and isobutyl propionate, suggesting the minimal loss of the GH-original flavor substances caused by IST. Lower contents of diallyl sulfide and acetic acid compared with other accelerated samples could be attributed to the sterilization effect of 8 kGy irradiation. However, IST induced a sharp increase in (E, E)-2,4-hexadienal, as a specific irradiation VOC product reported previously in strawberries with 4 kGy ^{60}Co-γ irradiation[42]. The remarkable increase of benzaldehyde, 2-furaldehyde, and 2-acetylfuran detected in IST samples, being similar to irradiation 'aftereffects' reported previously[43], indicated that IST may exert delayed promoting effects on VOCs consistent with Maillard-related pathways. However, these irradiation-specific components showed no significant impact on GH flavors due to their low contribution.

Correlation analyses based on multi-omics

For VCT samples (Fig. 6a), VCT-induced change in VOCs was accompanied by bacterial and fungal community shift. Briefly, 6-oxoheptanoic acid was positively correlated (> 0.9) with *Enterobacteriaceae*, *Saccharomyces* sp., *Bionectria solani*, and *Microdochium bolleyi*, while 2-octylcyclopropene-1-heptanol and 2,6-dimethyl-2,7-octadiene-1,6-diol were both positively correlated (> 0.9) with *Segatella*, *Enterobacteriaceae*, *Saccharomyces* sp., *B. solani*, *Sclerotiniaceae*, and *M. bolleyi*, and acetic acid was positively correlated with (> 0.9) *Weissella* and an unclassified *Nectriaceae*. This phenomenon indicated the potential effect of microbial activities on unpleasant VOC accumulation. In contrast, several GH-characteristic flavor-contributing VOCs showed significant negative correlations with (< −0.9) specific microorganisms. Isophorone was negatively correlated were negatively correlated with (< −0.9) *Enterobacteriaceae*, *Saccharomyces* sp., *B. solani*, and *M. bolleyi*, while phenethyl alcohol and ethyl palmitate with (< −0.9) *Weissella* and *Nectriaceae*; and (E)-linalool oxide (furanoid) with (< −0.9) *Saccharomyces* sp. These relationships are consistent with the reduction of GH-specific aroma compounds after VCT (Fig. 3f). These results suggest that VCT not only caused physical loss of highly volatile GH-characteristic aroma compounds, but also generated a stronger coupling between microbial community shifts and VOC changes, leading to a mixed aroma profile characterized by loss of floral/woody/cooling notes and microbial-associated accumulation of unfavorable or altered volatiles.

For 8 kGy γ-irradiated samples (Fig. 6b), the microbe–VOC association pattern was clearly different from that of VCT. Some unfavorable VOCs still showed positive correlations with (> 0.9) a limited number of microbial taxa: 6-oxoheptanoic acid was positively correlated with *Archaeorhizomyces* sp., and 2-octylcyclopropene-1-heptanol was positively correlated with *Segatella*, *Aspergillus spiculosus*, *Archaeorhizomyces* sp., and *Linnemannia camargensis*. However, 2,6-dimethyl-2,7-octadiene-1,6-diol did not show a clear, highly significant positive correlation. More importantly, the key GH-characteristic flavor compounds retained by γ-irradiation, including phenethyl alcohol, isophorone, and (E)-linalool oxide (furanoid), did not show extensive highly significant negative correlations with (< −0.9) bacterial or fungal taxa. This supports the conclusion that γ-irradiation helped maintain these characteristic floral, woody, and cooling aroma compounds with weaker dependence on microbial community variation. In addition, several pleasant VOCs showed positive correlations with (> 0.9) selected microorganisms: ethyl acetate was positively correlated with *Leuconostoc* and *Segatella*; ethyl isovalerate was positively correlated with *Bacteroides*, *Lactococcus*, *Lacticaseibacillus*, *Agathobacter*, and *Alternaria*; 2-butanone was positively correlated with *Clostridium*, *Lactococcus*, *Bifidobacterium*, an unclassified *Ruminococcaceae*, *Agathobacter*, and *Weissella*; 2-propanone was positively correlated with *Enterococcus*, *Bacteroides*, and an unclassified *Alternaria*; and 1-hydroxy-2-propanone was positively correlated with *Liquorilactobacillus*, *Weizmannia*, an unclassified *Ruminococcaceae*, and *Weissella*. These results indicated that γ-irradiation did not completely eliminate microbe–VOC associations, but these associations were more selective and did not strongly involve the major retained GH-characteristic aroma compounds. Therefore, compared with VCT, 8 kGy γ-irradiation appears to better preserve the characteristic aroma profile of GH while reducing the broad microbial coupling associated with aroma deterioration.

Conclusions

In conclusion, the geographically indicated agricultural product GH possessed phenylacetaldehyde, isophorone, phenylethanol, dodecanal, lilac aldehyde, and esters as primary flavor substances showing characteristic strong cooling sensation, with *Apilactobacillus* and *Bombella* as main probiotics. γ-Irradiation (8 kGy), rather than simply moisture control by vacuum concentration, was confirmed to effectively inhibit the proliferation of potentially undesirable taxa, including *Enterococcus*, *Methylobacterium*, *Clostridium*, *Faecalibacterium*, and osmotolerant yeasts, while maintaining the GH-characteristic fragrance substances. γ-Irradiation inhibited several undesirable VOCs probably associated with microbial or enzymatic transformation, although showing increased levels of several VOCs associated with oxidation- and Maillard-related pathways. Thus, γ-irradiation was considered to be an effective and promising non-thermal strategy for honey and honey-containing products sterilization, causing no significant damage to post-storage sensory qualities.

Ethical statements

This research was conducted in accordance with the Declaration of Helsinki. All panelists were fully informed of the study's purpose, procedures, and voluntary nature prior to participation. Informed consent was obtained from each panelist by signing a written consent form, and measures were taken to ensure the confidentiality of their personal information. No potential risks or discomforts were associated with participation in this study.

Author contributions

The authors confirm their contributions to the paper as follows: resources: Yang X, Zhong K, Wang Z; methodology: Zhou X, Mo X, Yang X, Zhong K, Wang Z, Duan F; investigation: Zhou X, Mo X, Yang X; supervision: Zhong K, Wang Z, Jia L; data curation: Zhou X, Xu W, Li Y; software: Xu W; formal analysis: Li Y; visualization and writing-original draft: Zhou X; writing-review & editing: Duan F, Sun Q; funding acquisition and project administration: Duan F. All authors reviewed the results and approved the final version of the manuscript.

Data availability

The raw data of 16S rRNA and ITS amplicon sequencing obtained in this study have been submitted to NCBI (National Center for Biotechnology Information) under accession number PRJNA1457969. GC-MS/GC-IMS feature tables are provided in the supplementary materials. Other datasets are available from the corresponding author upon reasonable request.

Acknowledgments

This work was supported by the National Natural Science Foundation of China (Grant No. 32102109), the Fundamental Research Funds for the Central Universities, Sichuan University-Dazhou special fund, China (Grant No. 2021CDDZ-17).

Conflict of interest

The authors declare that they have no known competing financial interests or personal relationships that could have appeared to influence the work reported in this paper.

Supplementary information accompanies this paper online at: https://doi.org/10.48130/fia-0026-0046.

Dates

Received 4 January 2026; Revised 4 July 2026; Accepted 23 August 2026; Published online 30 October 2026

References

[1] Li N, Song M, Li H, Liu Z, Jiang A, et al. 2024. Advancement of foodomics techniques for honey botanical origins authentication: past decade (2013–2023) and future perspectives. *Trends in Food Science & Technology* 147:104458

[2] Bhure RA, Alam M, Nanda V, Pawar VM, Saxena S. 2025. Exploring the impact of thermal processing on the quality attributes of honey: a comprehensive review. *Journal of Food Process Engineering* 48:e70033

[3] Mo X, Zhou X, Chen Y, Yang C, Gong M, et al. 2025. Chemical composition profiles of *Apis cerana* fabr. produced Acacia honey: a comparative study on optimal non-acidified ACN extraction with water-dilution by widely targeted metabolomics. *European Food Research and Technology* 251:2699–2717

[4] Hossain ML, Lim LY, Hammer K, Hettiarachchi D, Locher C. 2023. Monitoring the release of methylglyoxal (MGO) from honey and honey-based formulations. *Molecules* 28:2858

[5] Kędzierska-Matysek M, Teter A, Daszkiewicz T, Florek M. 2023. Microbiological quality of Polish artisanal varietal honeys. *Foods* 12:3349

[6] Sharma A, Pant K, Brar DS, Thakur A, Nanda V. 2023. A review on Apiproducts: current scenario of potential contaminants and their food safety concerns. *Food Control* 145:109499

[7] Al-Waili N, Salom K, Al-Ghamdi A, Ansari MJ. 2012. Antibiotic, pesticide, and microbial contaminants of honey: human health hazards. *The Scientific World Journal* 2012:930849

[8] Vázquez-Quiñones CR, Moreno-Terrazas R, Natividad-Bonifacio I, Quiñones-Ramírez EI, Vázquez-Salinas C. 2018. Microbiological assessment of honey in México. *Revista Argentina de Microbiología* 50:75–80

[9] Snowdon JA, Cliver DO. 1996. Microorganisms in honey. *International Journal of Food Microbiology* 31:1–26

[10] Santos-Buelga C, González-Paramás AM. 2017. Chemical composition of honey. In *Bee Products - Chemical and Biological Properties*, ed. Alvarez-Suarez JM. Cham: Springer International Publishing. pp. 43–82 doi: 10.1007/978-3-319-59689-1_3

[11] Xiong ZR, Sogin JH, Worobo RW. 2023. Microbiome analysis of raw honey reveals important factors influencing the bacterial and fungal communities. *Frontiers in Microbiology* 13:1099522

[12] Brudzynski K. 2021. Honey as an ecological reservoir of antibacterial compounds produced by antagonistic microbial interactions in plant nectars, honey and honey bee. *Antibiotics-Basel* 10:551

[13] Jaradat Z, Khataybeh B, Al Ghzawi AM, Ababneh Q, Al Nabusli A. 2022. Molecular identification of major bacteria in honey and the effect of microwave treatment on its microbial quality and antibacterial activity. *AIMS Agriculture and Food* 7:594–613

[14] Ravindran R, Jaiswal AK. 2019. Wholesomeness and safety aspects of irradiated foods. *Food Chemistry* 285:363–368

[15] Klutse CK, Larbi DA, Adotey DK, Serfor-Armah Y. 2021. Assessment of effect of post-harvest treatment on microbial quality of honey from parts of Ghana. *Radiation Physics and Chemistry* 182:109368

[16] Osterholm MT, Norgan AP. 2004. The role of irradiation in food safety. *New England Journal of Medicine* 350:1898–1901

[17] Khalil MI, Islam MA, Alam N, Gan SH, Sulaiman SA. 2015. Irradiation and evaporation enhance physicochemical characteristics, AEAC, FRAP, protein and proline contents of Tualang honey. *Journal of Food Biochemistry* 39:742–753

[18] Liu S, Dong H, Lu H, Li Y, Zhang G, et al. 2025. Dynamic changes in composition during processing of *Lonicerae japonicae* flos black tea. *Food Chemistry* 493:145684

[19] Xu N, Tan G, Wang H, Gai X. 2016. Effect of biochar additions to soil on nitrogen leaching, microbial biomass and bacterial community structure. *European Journal of Soil Biology* 74:1–8

[20] Gardes M, Bruns TD. 1993. ITS primers with enhanced specificity for basidiomycetes – application to the identification of mycorrhizae and rusts. *Molecular Ecology* 2:113–118

[21] Kardas M, Staśkiewicz-Bartecka W, Sołtys K, Dul L, Sapała AM, et al. 2023. The quality of selected raw and pasteurized honeys based on their sensory profiles and consumer preferences. *Frontiers in Nutrition* 10:1330307

[22] Lin C, Chen C, Liu Y, Liu R, Lu Q. 2025. Characterization and discrimination of *Rhus chinensis* Mill. honeys from different geographical origins based on physicochemical parameters, minerals, volatile compounds and antioxidant activities. *Journal of Food Measurement and Characterization* 19:3581–3599

[23] Dobre I, Alexe P, Escuredo O, Seijo CM. 2013. Palynological evaluation of selected honeys from Romania. *Grana* 52:113–121

[24] Azonwade FE, Paraïso A, Agbangnan Dossa CP, Dougnon VT, N'tcha C, et al. 2018. Physicochemical characteristics and microbiological quality of honey produced in Benin. *Journal of Food Quality* 2018:1896057

[25] Maeno S, Endo A. 2024. Inconsistent identification of *Apilactobacillus kunkeei*-related strains obtained by well-developed overall genome-related indices. *Systematic and Applied Microbiology* 47:126559

[26] Härer L, Hilgarth M, Ehrmann MA. 2022. Comparative genomics of acetic acid bacteria within the genus *Bombella* in light of beehive habitat adaptation. *Microorganisms* 10:1058

[27] Echegaray N, Yilmaz B, Sharma H, Kumar M, Pateiro M, et al. 2023. A novel approach to *Lactiplantibacillus plantarum*: from probiotic properties to the omics insights. *Microbiological Research* 268:127289

[28] Calatrava E. 2022. Other *Streptococcus* species and *Enterococcus*. In *Encyclopedia of Infection and Immunity*, ed. Rezaei N. Amsterdam: Elsevier. pp. 529–541 doi: 10.1016/b978-0-12-818731-9.00159-2

[29] Kovaleva J, Degener JE, van der Mei HC. 2014. *Methylobacterium* and its role in health care-associated infection. *Journal of Clinical Microbiology* 52:1317–1321

[30] Liang D, Cui X, Li M, Zhu Y, Zhao L, et al. 2023. Effects of sporulation conditions on the growth, germination, and resistance of *Clostridium*

perfringens spores. *International Journal of Food Microbiology* 396:110200

[31] Niyomvong N, Trakunjae C, Boondaeng A. 2023. Fermentation characteristics and aromatic profiles of plum wines produced with *Hanseniaspora thailandica* Zal1 and common wine yeasts. *Molecules* 28:3009

[32] Bullerman LB. 2003. SPOILAGE | fungi in food – an overview. In *Encyclopedia of Food Sciences and Nutrition*, ed. 2nd Edition. Caballero B. Amsterdam: Elsevier. pp. 5511–5522 doi: 10.1016/b0-12-227055-x/01129-9

[33] Praphailong W, Fleet GH. 1999. *DEBARYOMYCES*. In *Encyclopedia of Food Microbiology*, ed. Robinson RK. Amsterdam: Elsevier. pp. 515–520 doi: 10.1006/rwfm.1999.0430

[34] Moreira RFA, De Maria CAB, Pietroluongo M, Trugo LC. 2010. Chemical changes in the volatile fractions of Brazilian honeys during storage under tropical conditions. *Food Chemistry* 121:697–704

[35] Bock G, Benda I, Schreier P. 1986. Biotransformation of linalool by *Botrytis* cinerea. *Journal of Food Science* 51:659–662

[36] Pinheiro L, Marsaioli AJ. 2007. Microbial monooxygenases applied to fragrance compounds. *Journal of Molecular Catalysis B: Enzymatic* 44:78–86

[37] Wang Z, Ma Y, Zhao G, Liao X, Chen F, et al. 2006. Influence of gamma irradiation on enzyme, microorganism, and flavor of cantaloupe (*Cucumis melo* L.) juice. *Journal of Food Science* 71:M215–M220

[38] Chernetsova ES, Morlock GE. 2012. Assessing the capabilities of direct analysis in real time mass spectrometry for 5-hydroxymethylfurfural quantitation in honey. *International Journal of Mass Spectrometry* 314:22–32

[39] Wang Y, Rodolfo Juliani H, Simon JE, Ho CT. 2009. Amino acid-dependent formation pathways of 2-acetylfuran and 2,5-dimethyl-4-hydroxy-3[2H]-furanone in the Maillard reaction. *Food Chemistry* 115:233–237

[40] Liu Y, Li J, Cheng Y, Liu Y. 2019. Effect of frying oils' fatty acid profile on quality, free radical and volatiles over deep-frying process: a comparative study using chemometrics. *LWT* 101:331–341

[41] Qian M, Zheng M, Zhao W, Liu Q, Zeng X, et al. 2021. Effect of marinating and frying on the flavor of braised pigeon. *Journal of Food Processing and Preservation* 45:e15219

[42] Yao S, Chen SQ, Zhou GW, Luo J, Xu X, et al. 2018. Effect of ^{60}Co-γ irradiation treatment on color, flavor and firmness of strawberry fruit during storage. *Science and Technology of Food Industry* 39:254–259 (in Chinese)

[43] Thakur BR, Singh RK. 1994. Food irradiation - chemistry and applications. *Food Reviews International* 10:437–473

Copyright: © 2026 by the author(s). Published by Maximum Academic Press on behalf of China Agricultural University, Zhejiang University and Shenyang Agricultural University. This article is an open access article distributed under Creative Commons Attribution License (CC BY 4.0), visit https://creativecommons.org/licenses/by/4.0/.